SIGNIFICANCE OF THE WEIBULL DISTRIBUTION AND ITS SUB-MODELS IN NATURAL IMAGE STATISTICS

Victoria Yanulevskaya, Jan-Mark Geusebroek
Intelligent Systems Lab Amsterdam, Informatics Institute, University of Amsterdam, Kruislaan 403, Amsterdam, The Netherlands
V.Yanulevskaya@uva.nl, Geusebroek@uva.nl

Keywords: Natural image statistics, Weibull distribution, model selection.

Abstract: The contrast statistics of natural images can be adequately characterized by a two-parameter Weibull distribution. Here we show how distinct regimes of this Weibull distribution lead to various classes of visual content. These regimes can be determined using model selection techniques from information theory. We experimentally explore the occurrence of the content classes, as related to the global statistics, local statistics, and to human attended regions. As such, we explicitly link local image statistics and visual content.

1 INTRODUCTION

While looking at the world around us, we see a wide variety of images. These images, being a visual projection of the world on our eye, are not random, but highly organized and structured. This is reflected in the statistics of natural images. With natural images, we mean real-world photos, including both natural landscapes and man-made environments. Surprisingly, the contrast statistics of such natural images can be adequately described by a simple model (Geusebroek & Smeulders, 2003).

Natural image statistics have widely been studied in the field of image coding (Field, 1987), image compression and image representation (Mallat, 1989), and more recently, in 3D scene geometry understanding (Nedovic et al., 2007), visual categorization (Oliva & Torralba, 2001). Despite its apparent importance, not many efforts have been undertaken to gain a fundamental insight in understanding the cause and significance of these statistics.

One of the most important image statistics is the distribution of contrasts. Mallat (1989) and later Simoncelli (1999) propose the generalized Laplacian distribution as a parameterized model which provides a good fit to the statistics of natural images. Huang and Mumford (1999) systematically investigate various statistical properties of natural images on a large calibrated image database (van Hateren, 1998). They confirm that the statistics involving linear filters can be modeled by a generalized Laplacian distribution. Geusebroek and Smeulders (2005) generalize these findings in showing that the dominant distribution of texture statistics follows the Weibull distribution. An overview of statistical modelling of natural images can be found in Srivastava et al. (2003).

Scholte et al. (2008) examined to which degree the brain is sensitive to these natural image statistics, by considering the ERP brain measurements of human subjects. They found a correlation of 84% and 93% between the Weibull parameters as derived from images and a simple model of ERP measurements obtained from the parvo- and magnocellular system. Given these results, one would expect the Weibull distribution to play a significant role in image statistics.

The central question we address in this paper is: *In how far can natural image statistics explain visual content?* To address this question, we explore edge distributions of natural images at the global and local level. We distinguish four classes of natural images according to the behavior of the Weibull distribution. As we will show, each class seems to reflect a specific type of visual content. Furthermore, we study the occurrence of the different classes for human attended regions.

Novel in our approach is the explicit link between regional statistics and visual content, as reflected in the Weibull sub-models. Furthermore, from a human

attention perspective we study the importance of each sub-model.

The paper is organized as follows. Section 2 introduces the integrated Weibull distribution to capture the natural image statistics. The maximum likelihood estimators of the Weibull parameters are provided. Furthermore, we distinguish four different sub-models of the Weibull distribution, and apply information theory to differentiate these sub-models. We present the g-test as a goodness of fit test between the data and the Weibull distribution. In Section 3 we explore the occurrence of the different sub-models of the Weibull distribution on an image data set, and we link the sub-models to the visual content. We consider three experiments. We start by analyzing the statistics of the whole image. Then we zoom in on the local image statistics. Finally, we explore the statistics of human attended regions. We wrap up with conclusions in Section 4.

2 IMAGE STATISTICS

The parameterized model which provides a good fit to the edge distribution of natural images (Geusebroek & Smeulders, 2003; Simoncelli, 1999; Huang & Mumford, 1999) has a probability density function (pdf) given by,

$$p(x) = \frac{\gamma}{2\gamma^{\frac{1}{\gamma}}\beta\Gamma(\frac{1}{\gamma})} \exp\left(-\frac{1}{\gamma}\left|\frac{x}{\beta}\right|^{\gamma}\right), \qquad (1)$$

where x is the edge response to the Gaussian derivative filter, $\gamma > 0$ is the shape parameter and $\beta > 0$ is the scale parameter of the distribution. $\Gamma(\cdot)$ is the complete Gamma function,

$$\Gamma(x) = \int_0^{\infty} t^{x-1}\exp^{-t}dt. \qquad (2)$$

Through out the paper we will refer to this model as the two parameter integrated Weibull distribution, considering its close relationship to the Weibull distribution (Geusebroek & Smeulders, 2003). The parameter β denotes the width of the distribution and the parameter γ represents the peakness of the distribution. The width β reflects the local contrast. A wide distribution indicates a texture with high contrast. The shape γ is sensitive to the local edge spatial frequency. These two parameters catch the structure of the image texture (Geusebroek & Smeulders, 2005). Figure 1 illustrates the integrated Weibull pdf for some example images.

The integrated Weibull distribution captures the behavior of other statistical distributions, mainly being the power-law, exponential, and gaussian distribution. Our aim is to explore the link between the

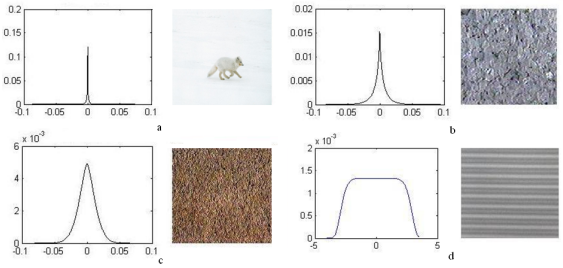

Figure 1: Integrated Weibull PDF's for different kind of textures: object-background image (a), images with moderate contrast content (b), high-frequency texture image (c) and image with a regular pattern (d).

Weibull statistics and visual content. Hence, besides investigating the variation in image content as function of the Weibull parameters by means of scatter plots, we will explore visual content by categorizing these statistical sub-models. To distinguish between the different sub-models, we need to know parameters of each model. They can be estimated with the Maximum Likelihood Estimation (MLE) technique. After that, we can quantify the various sub distributions using model selection techniques.

2.1 Maximum likelihood estimation

The likelihood function indicates how well a distribution describes the observed data $X = x_1, x_2, ..., x_n$. The best fit is obtained when model parameters maximize the log-likelihood function, in which case their respective derivatives should equal zero. For the integrated Weibull distribution given by Eq.(1), the best fit is obtained when

$$\frac{\partial}{\partial\beta}\ln L_{iw}(\beta,\gamma|X) = -\frac{1}{\beta} + \frac{1}{\beta}\sum_{i=1}^{n}\left|\frac{x_i}{\beta}\right|^{\gamma} = 0, \qquad (3)$$

and

$$\begin{aligned}\frac{\partial}{\partial\gamma}\ln L_{iw}(\beta,\gamma|X) &= \frac{1}{\gamma^2}\left(\gamma - 1 + \psi\left(\frac{1}{\gamma}\right) + \right.\\ &\quad \left. + \ln(\gamma) + \sum_{i=1}^{n}\left|\frac{x_i}{\beta}\right|^{\gamma}\right) - \\ &\quad \frac{1}{\gamma}\sum_{i=1}^{n}\left|\frac{x_i}{\beta}\right|^{\gamma}\ln\left|\frac{x_i}{\beta}\right| = 0, \qquad (4)\end{aligned}$$

where,

$$\psi(\gamma) = \frac{d}{d\gamma}\ln\Gamma(\gamma) = \frac{\frac{d}{d\gamma}\Gamma(\gamma)}{\Gamma(\gamma)} \qquad (5)$$

is the digamma function.

The parameter γ is obtained by eliminating β from Eq. (4):

$$f(\gamma,X) = -\frac{1}{\gamma}\sum_{i=1}^{n}\frac{|x_i|^\gamma}{\sum_{i=1}^n|x_i|^\gamma}\ln\frac{|x_i|^\gamma}{\sum_{i=1}^n|x_i|^\gamma}+ 1+\frac{1}{\gamma}\ln(\gamma)+\frac{1}{\gamma}\psi\left(\frac{1}{\gamma}\right)=0. \quad (6)$$

Eq. (6) may be solved using standard iterative procedures, for example, the Newton-Raphson method:

$$\gamma_{k+1} = \gamma_k - \frac{f(\gamma_k)}{\frac{\partial}{\partial\gamma}f(\gamma_k)},$$
$$\frac{\partial}{\partial\gamma}f(\gamma,X) = \sum_{i=1}^{n}\Lambda\frac{\sum_{i=1}^n x_i^\gamma}{x_i^\gamma} - n\sum\Lambda - n\sum_{i=1}^{n}\Lambda\ln\left(\frac{x_i^\gamma n}{\sum_{i=1}^n x_i^\gamma}\right), \quad (7)$$

where

$$\Lambda = \frac{\partial}{\partial\gamma}\left(\frac{x_i^\gamma}{\sum_{i=1}^n x_i^\gamma}\right). \quad (8)$$

The Newton-Raphson algorithm works as shown in Alg. 1. Thus, the maximum likelihood estimator $\hat{\gamma}$ is the solution of Eq. (6) and then $\hat{\beta}$ can be calculated from Eq. (3), until convergence.

Algorithm 1 Integrated Weibull parameter estimation

$\gamma = 1$ *initial value*
$\varepsilon = 0.001$ *accuracy of the calculations*
$\gamma_{next} = \gamma - \frac{f(\gamma,X)}{\frac{\partial}{\partial\gamma}f(\gamma,X)}$
while $|\gamma_{next} - \gamma| > \varepsilon$
  $\gamma = \gamma_{next}$
  $\gamma_{next} = \gamma - \frac{f(\gamma,X)}{\frac{\partial}{\partial\gamma}f(\gamma,X)}$
return γ_{next}.

MLE for parameters of the power law, the exponential, and the Gaussian distribution are well known and can be easily calculated. Their pdf's are given by

$$P(x) = \frac{\beta}{2a}\left|\frac{x}{a}\right|^{\beta-1}, \quad (9)$$
$$E(x) = \frac{1}{2\beta}\exp\left(-\left|\frac{x}{\beta}\right|\right), \quad (10)$$
$$G(x) = \frac{1}{\sqrt{2\pi\beta}}\exp\left(-\frac{x^2}{2\beta^2}\right). \quad (11)$$

The corresponding maximum likelihood estimations are

$$\hat{\beta}_p = \frac{n}{-\sum_{i=1}^n\log(|\frac{x_i}{a}|)}, \quad (12)$$
$$\hat{\beta}_e = \frac{\sum_{i=1}^n|x_i|}{n}, \quad (13)$$
$$\hat{\beta}_g = \frac{\sum_{i=1}^n(x_i)^2}{n}. \quad (14)$$

2.2 Model selection

We use Akaike's information criterion (AIC) (Akaike, 1973) for appropriate model selection. AIC estimates expected Kullback-Leibler information, based on the log-likelihood function at its maximum point. Hence, we do not need to assume that the "true model" is in the set of candidates (Burnham & Anderson, 2004). AIC for model i is

$$AIC_i = -\log(L_i(\hat{\beta}_i|X)) + K_i, \quad (15)$$

where L_i is the likelihood function of the model i, $\hat{\beta}_i$ is the maximum likelihood estimator of the model parameters based on the assumed model i and the data X, and K_i is the number of parameters of the model i. In our case, parameter $\hat{\beta}_i$ is defined by Eq. (12)-(14) for each particular model. In the end we have three AIC values corresponding to the power law, the exponential, and the Gaussian distribution. The best model is the one with minimum value AIC_{min}. However, we follow (Burnham & Anderson, 2002) and assign a probability to each model by

$$w_i = \frac{\exp(-\Delta_i/2)}{\Sigma_{r=1}^R\exp(-\Delta_r/2)}, \quad (16)$$

where

$$\Delta_i = AIC_i - AIC_{min} \quad (17)$$

and R is the number of models, $R = 3$ in our case. The w_i are called Akaike weights and are interpreted as a probability that model i fits the data X best over the considered set of models.

2.3 g-Test

Sometimes none of the considered models represents the data appropriately. Thus, it should be tested how well the integrated Weibull distribution fits the data. The g-test is the log-likelihood equivalent of the chi-squared test, given by:

$$g = 2\sum_{j=1}^{k}O_j\log\left(\frac{O_j}{E_j}\right), \quad (18)$$

where O_j is the number of observed values x_i in bin j of the histogram of the data X. Furthermore, E_j is

a number of expected values in the same bin j under the fitted distribution. The hypothesis that the distribution is of a given form is accepted if the calculated test statistic g is less than an appropriate critical value. The g-test can be applied with the same critical values as the chi-squared test. In this paper we use a critical value which corresponds to a significance level of $\alpha = 0.05$ and 100 degrees of freedom ($g < 77.929$) (Filliben, 2002).

2.4 The four regimes of the integrated Weibull distribution

We can now distinguish four types of natural images according to the behavior of the integrated Weibull distribution. When the integrated Weibull distribution fits the data well, its sub-models define the first three types, being: the power law, the exponential or the Gaussian. The fourth type of natural images occurs when the integrated Weibull distribution does not describe the data well. Our aim is to assign one particular type to a (sub-)image.

3 EXPERIMENTS

To illustrate the different regimes of the integrated Weibull distribution, we analyze a data set containing 107 natural images of size 800x540 pixels. These images are selected from three categories of National Geographic wallpapers[1]: animals, landscapes, and people. We are interested in the intensity edge distribution and its sub-models according to the four regimes of the integrated Weibull distribution. To obtain the intensity edge distribution, we do not use the standard edge filters, e.g. Sobel style, instead we apply the Gaussian derivative filter ($\sigma = 1$) and steer it in the gradient direction. Then we consider a histogram (101 bins) of the responses, and fit the integrated Weibull distribution to this histogram. Finally, we select the appropriate sub-model using Akaike's information criterion.

3.1 Global image statistic analysis

We start by analyzing the presence of the various integrated Weibull sub-models in the statistics of the whole image. We extract edges and study their distribution globally for each image from the data set. The results are shown in Table 1.

All images fit well to the integrated Weibull distribution according to the g-test ($\alpha = 0.05$). Power law distribution is chosen as an appropriate sub-model for 20% of the images. These images have well separated foreground and uniform background regions, see Figure 2(a). Only 2% of the images are Gaussian distributed, these are images which contain mostly high-frequency texture, illustrated in Figure 2(c). Most of the images (78%) follow the exponential distribution, which refers to moderate contrast contents. These images usually contain a lot of details at different scales, see Figure 2(b).

Table 1: Four regimes of the integrated Weibull distribution for global image analysis.

Int. Weibull			Not Int. Weibull
100%			0%
Power Law	Exp.	Gauss.	-
20%	78%	2%	-

Figure 3 gives an overview of the occurrence of each sub-model in the entire image collection. Each of the sub-models indicates different image content. Images with strong object-background contrasts are close to the power law behavior. Images with moderate contrast tend to follow the exponential distribution. High-frequency texture images are described by the Gaussian distribution.

(a) (b) (c)

Figure 2: Typical images for three sub-models of the integrated Weibull distribution. Figure (a) corresponds to the power law sub-model, (b) and (c) show, respectively, examples for the exponential and the Gaussian sub-models.

3.2 Local image statistic analysis

Edge distributions of natural images follow the integrated Weibull when looking at global statistics as shown above. More important, the various sub-models of the integrated Weibull distribution seem to reflect visual content. One would expect this effect to be even stronger when considering local patches, as local visual content is more coherent. Therefore, for the local analysis, we divide images into rectangular patches (60x60 pixels) and consider the edge histogram and model selection over these patches.

Results are presented in Table 2. For experimental setup reasons (see below), we consider a subset of 49 images, however, results for the whole data set

[1] http://www.nationalgeographic.com/

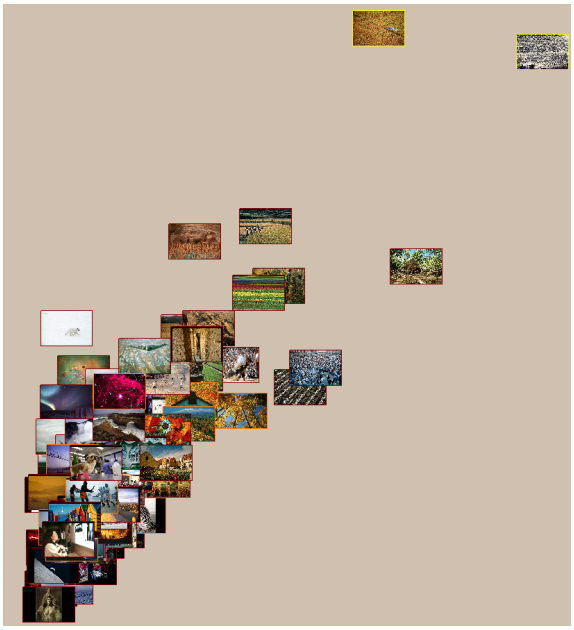

Figure 3: Scatter plot of integrated Weibull parameters β and γ with each image positioned at its respective (β,γ) values. The horizontal axis represents the value of the β parameter, indicating contrast. The vertical axis represents value of the γ parameter (between 0 and 3). A red frame indicates the image is fitted by the power law distribution. Images with blue frames follow the exponential distribution. Yellow framed images are described with the Gaussian distribution.

are similar (data not shown). Comparing these results with the global analysis (Table 1), local patches do not always follow the integrated Weibull distribution according to the g-test ($\alpha = 0.05$). For one, regions without edges are dominated by compression artifacts and may not follow the integrated Weibull distribution. Furthermore, in many cases, patches are composed of a few parts, each following a different sub-model. Thus, each part seems to conform the integrated Weibull distribution, but all together they do not follow one of the sub-models. In the global analysis, we have the same situation, where images are composed of many parts due to objects and clutter. However, the resulting distribution of the whole image combines into the exponential distribution due to the large amount of parts (Burghouts et al., 2007). This explains the smaller portion of local patches described with the exponential sub-model in comparison with the global analysis.

The Gaussian sub-model occurs more often at local scale. The Gaussian distribution describes uniform regions of high-frequency textures. Images containing only high-frequency textures are rather rare in a photo stock. However, uniform textured regions do occur in images, and local analysis reflects this. Comparing the results for the power law sub-model, the model behaves relatively similar at the global and local levels.

Table 2: Four regimes of the integrated Weibull distribution for local region analysis.

Int. Weibull			Not int. Weibull
87%			13%
Power Law	Exp.	Gauss.	-
26%	47%	14%	-

Figure 4 illustrates how the patch's visual content is reflected by the integrated Weibull sub-models. The figure represents a scatter plot of integrated Weibull parameters β and γ with each patch positioned at its respective (β,γ) value. The power law sub-model is concentrated at the bottom which corresponds to small γ values ($\gamma < 1$). This sub-model is linked to the patches containing uniform regions separated by strong edges, but are not very detailed, as shown in the inset. The exponential sub-model spans a wide range of γ values, starting within the power law sub-model, and ending at the lower regions of the Gaussian sub-model. This sub-model corresponds to γ values around 1 and describes more detailed patches. The Gaussian sub-model ends up at the top of the figure, where the γ parameter is close to 2. High-frequency with high contrast patches are reflected in the Gaussian sub-model, as well as smoothed patches with Gaussian noise.

3.3 Attention based analysis of local image statistics

Visual content is closely connected to human attention while observing the world around us. Our visual system samples the environment not randomly, but is driven by visual stimuli, like variations in contrast or color (Baddeley & Tatler, 2006; Itti et al., 1998; Mante et al., 2005; Reinagel & Zador, 1999). We are interested in the occurrence of various sub-models of the integrated Weibull distribution in the statistics of local regions attended by humans. To obtain the ground truth attended regions, human eye fixations were recorded for the subset of 49 images. Eighteen subjects participated in the experiment, they were shown each image for 5 seconds. For each fixation point we consider a fovea-sized patch (60x60 pixels). Again the local edge distribution analysis is applied for each fixated patch.

Based on the results shown in Table 3, we can con-

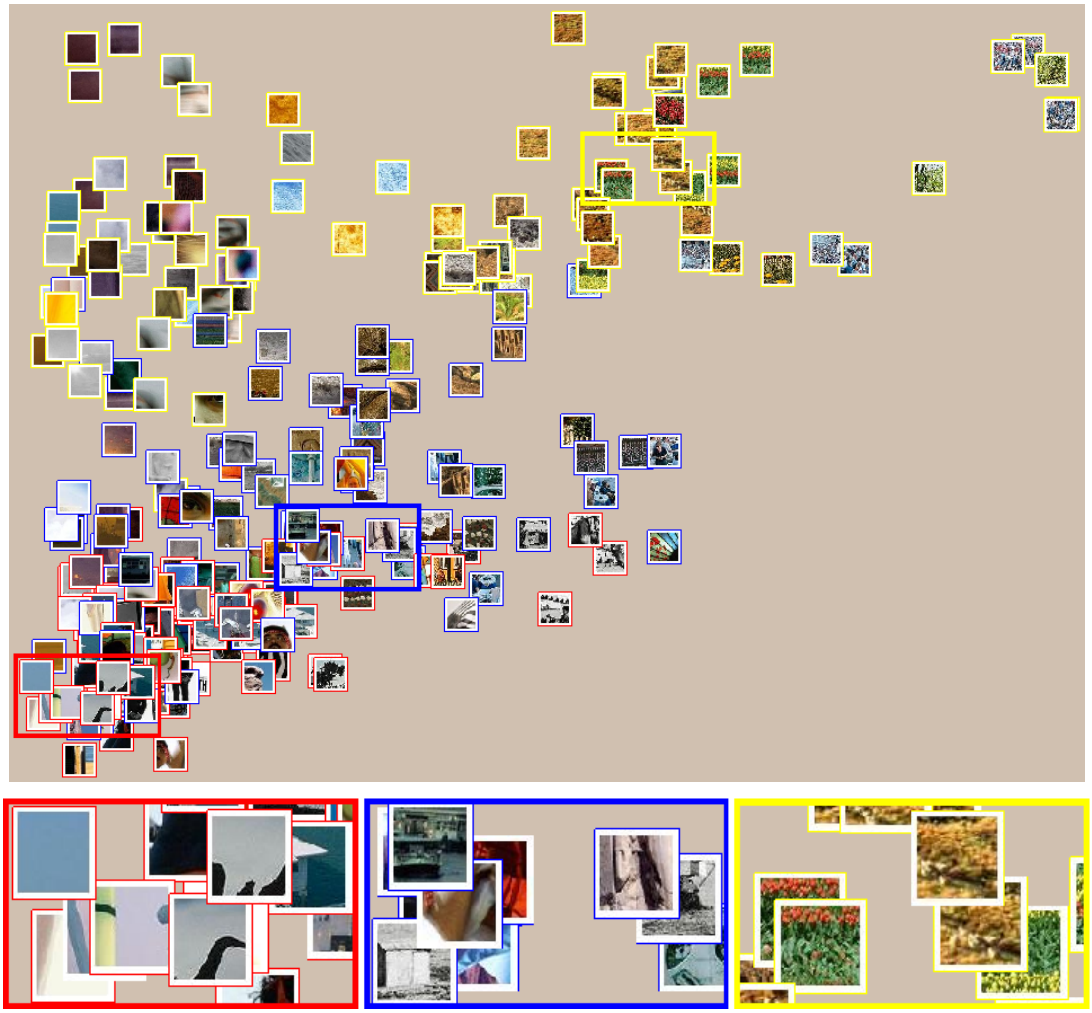

Figure 4: Scatter plot of integrated Weibull parameters β and γ with each patch positioned at its respective (β, γ) value. Again, the horizontal axis represents value of the β parameter, and the vertical axis represents value of the γ parameter (between 0 and 3). Red framed patches correspond to the power law sub-model. These patches contain uniform regions separated by strong edges, but are not very detailed, see the inset on the bottom left. Patches with blue frames follow the exponential distribution. Clearly they are showing more small scale details, as illustrated by the inset in the middle. Yellow framed patches are Gaussian distributed, there we observe two types of visual content. On the top right, high-frequency with high contrast patches are gathered, enlarged version is in the bottom right inset. On the top left, there are smooth patches with gaussian-like noise.

clude that attended regions differ from arbitrary selected local regions (Table 2). People tend to look to strong edges, which are power law distributed, in our results 33% for attended regions compared to 26% for arbitrary regions, respectively.

Table 3: Four regimes of the integrated Weibull distribution for attended region analysis.

Int. Weibull			Not int. Weibull
95%			5%
Power Law	Exp.	Gauss.	-
33%	55%	7%	-

Gaussian distributed patches occur more rare in attended regions in comparison with arbitrary regions, 7% versus 14%. The examples of Gaussian regions in Figure 4 (in yellow frames) show two types of Gaussian distributed patches. As one can notice, smooth patches with gaussian-like noise on the top left are not informative, thus, people generally do not fixate on such kind of regions. Instead, people look to detailed regions, which follow the exponential distribution. In our attention based analysis, the exponential sub-model is present in 55% of the results (Table 3), whereas this is only for 47% the case when considering arbitrary regions (Table 2). Regions which do not follow the integrated Weibull distribution according to the g-test, are less present in attended regions than in arbitrary regions, 5% versus 13%. This is may be due to the portion of regions without edge content as discussed previously.

Figure 5 illustrates the occurrence of different regimes of the integrated Weibull distribution with superimposed human gaze directions. As can be seen from the Figure, subjects seldom look to the Gaussian distributed regions, but prefer areas which follow the power law and the exponential distributions.

As discussed in Section 2, the integrated Weibull parameter β reflects the local contrast. From literature it is known that contrast plays an important role in human eye fixations (Reinagel & Zador, 1999; Baddeley & Tatler, 2006). Table 3.3 illustrates the mean values of the parameter β within each sub-model for arbitrary regions versus attended regions. The t-test shows that the local contrast captured by β is significantly higher ($p < 10^{-10}$ for each sub-model) in average for attended regions than for arbitrary regions. Therefore, our experiments reproduce the tendency of people to look at higher contrast regions. The results identify both contrast and edge frequency reflected in the integrated Weibull parameters and its sub-models might be cues for human attention.

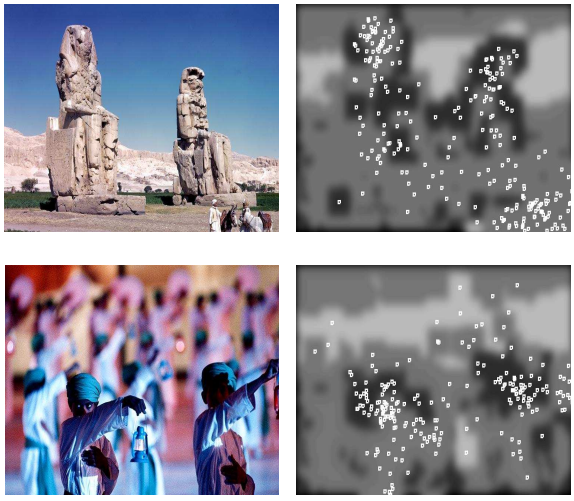

Figure 5: Visualization of the integrated Weibull sub-models with superposed human gaze directions. On the left two example images. On the right a visualization of the local model selection and the eye-tracking experiment. The black areas correspond to patches with power law sub-model, dark and light grey areas correspond to patches with the exponential and Gaussian sub-models, respectively. White small squares depict the human fixation points.

Table 4: Mean integrated Weibull β parameter.

	Power Law	Exp.	Gauss.
Arbitrary regions	0.0090	0.0149	0.0249
Attended regions	0.0119	0.0189	0.0287

4 CONCLUSIONS

In this paper, we have explored the link between visual content and natural image statistics modelled by the integrated Weibull distribution. We have given four different regimes with respect to the integrated Weibull distribution: power-law, exponential, Gaussian, and the case when the integrated Weibull distribution is not appropriate. With model selection techniques from information theory, we can determine the probability for every sub-model to explain the statistical properties of the regions. Our results show that natural image statistics explain a lot of visual content. Each sub-model reflects a specific type of visual content, at the global (see Figure 3), and at the local level (see Figure 4).

At the global level, all images from our collection follow the integrated Weibull distribution, see Table 1. Most of the images, around 80%, are exponentially distributed. The rest is mainly power law distributed, the Gaussian distribution being rare. In the local anal-

ysis we have considered the statistics of arbitrary and attended regions, see Tables 2 and 3, respectively. We have shown that the occurrence of the various sub-models in human attended versus arbitrary regions is significantly different. This might indicate a role of the Weibull sub-models in human attention.

In future work, we plan to address salient region detection algorithms based on these local image statistics. Furthermore, recent studies show natural image statistics play an important role in 3D scene perception (Pelli & Tillman, 2008). We plan to further exploit the various Weibull sub-models in condensed representations of 3D scenes.

References

Akaike, H. (1973). Information Theory and an Extension of the Maximum Likelihood Principle. *Int. Sympos. Inform. Theory* (pp. 267–281).

Baddeley, R. J. & Tatler, B. W. (2006). High frequency edges (but not contrast) predict where we fixate: A Bayesian system identification analysis. *Vision Res., 46(18)*, 2824–2833.

Burghouts, G. J., Smeulders, A. W. M. & Geusebroek, J. M. (2007). The distribution family of similarity distances. In *NIPS*.

Burnham, K. P. & Anderson, D. R. (2002). *Model selection and multimodel inference: A Practical Information-Theoretic Approach*. Springer.

Burnham, K. P. & Anderson, D. R. (2004). Multimodel Inference: Understanding AIC and BIC in Model Selection. *Sociological Methods & Research, 33(2)*, 261.

Field, D. J. (1987). Relations between the statistics of natural images and the response properties of cortical cells. *J. Opt. Soc. Am., 4*, 2370–2393.

Filliben, J. J. (2002). NIST/SEMATECH e-Handbook of Statistical Methods. http://www.itl.nist.gov/div898/handbook/. *NIST, Gaithersburg*.

Geusebroek, J. M. & Smeulders, A. W. M. (2003). Fragmentation in the vision of scenes. In *ICCV*.

Geusebroek, J. M. & Smeulders, A. W. M. (2005). A six-stimulus theory for stochastic texture. *Int. J. Comput. Vision, 62(1)*, 7–16.

van Hateren, J. H. (1998). Independent component filters of natural images compared with simple cells in primary visual cortex. *Biological Sciences, 265(1394)*, 359–366.

Huang, J. & Mumford, D. (1999). Statistics of natural images and models.

Itti, L., Koch, C. & Niebur, E. (1998). A model of saliency-based visual attention for rapid scene analysis. *Trans. Pattern Anal. Machine Intell., 20(11)*, 1254–1259.

Mallat, S. G. (1989). A theory for multiresolution signal decomposition: the wavelet representation. *Pattern Anal. Machine Intell., 11(7)*, 674–693.

Mante, V., Frazor, R. A., Bonin, V., Geisler, W. S. & Carandini, M. (2005). Independence of luminance and contrast in natural scenes and in the early visual system. *Nature Neurosci., 8(12)*, 1690–7.

Nedovic, V., Smeulders, A. W. M., Redert, A. & Geusebroek, J. M. (2007). Depth information by stage classification. In *ICCV*.

Oliva, A. & Torralba, A. (2001). Modeling the shape of the scene: A holistic representation of the spatial envelope. *Int. J. Comput. Vision, 42(3)*, 145–175.

Pelli, D. G. & Tillman, K. A. (2008). The uncrowded window of object recognition. *Nature Neurosc.* (p. to appear in october).

Reinagel, P. & Zador, A. (1999). Natural scene statistics at the centre of gaze. *Network: Comput. Neural Syst., 10(4)*, 341–350.

Scholte, H. S., Ghebreab, S., Smeulders, A. W. M. & Lamme, V. (2008). The parvo and magno-cellular systems encode natural image statistics parameters. *J. Vision, 8(6)*, 686a.

Simoncelli, E. P. (1999). Modeling the joint statistics of images in the wavelet domain. Volume 3813 (pp. 188–195).

Srivastava, A., Lee, A. B., Simoncelli, E. P. & Zhu, S. C. (2003). On Advances in Statistical Modeling of Natural Images. *J. Math. Imaging Vision, 18(1)*, 17–33.